

Evidence of rotational dependency on standard DTI measurements

Arturo Cardenas-Blanco¹, Julio Acosta-Cabronero¹, Martin Kanowski², Joern Kaufmann², Claus Tempelman², Stefan Teipel³, and Peter J Nestor¹

¹Brain plasticity and neurodegeneration, German Center for Neurodegenerative Diseases (DZNE), Magdeburg, Germany, ²Department of Neurology, Otto-von-Guericke University, Magdeburg, Germany, ³German Center for Neurodegenerative Diseases (DZNE), Rostock, Germany

Target audience: Neuroscientists and MR physicists interested in diffusion tensor imaging.

Purpose. Diffusion tensor imaging (DTI) has emerged as a research imaging technique with the potential to probe brain microstructure though methodological problems, in the form of technical inconsistencies at acquisition and/or analysis, can potentially lead to spurious results. The aim of this study was to challenge with two simple experiments the notion that standard DTI acquisition/processing strategies yield robust tensor estimates in the event of poor scan standardisation.

Methods. Experimental design. Two experiments (with phantom and human data) were designed to test the hypothesis that both field-of-view (FOV) and sample rotations can exert an undesirable influence on DTI measurements, with a view to highlighting the importance of standardising FOV and subject positioning in clinical studies. (i) Phantom study. In order to assess the impact of FOV rotations on fractional anisotropy (FA) estimates, N=18 scans were performed on a previously validated diffusion phantom¹: N=14 DTI measurements in straight (or true) axial orientation (TA) and N=4 with a 5-degree FOV rotation (TA-5) around X (i.e. around the scanner's left/right axis). (ii) Human study. To evaluate the combined effect on FA measurements of FOV and sample rotations, N=24 healthy subjects were scanned. The FOV in two N=8 groups of healthy volunteers (G1 and G2) were set to take relatively large angles ($\theta_{G1}=-23\pm 5$ degrees and $\theta_{G2}=-18\pm 3$ degrees with respect to the callosal axis across the midline (i.e. the line connecting the most inferior aspects of the mid-sagittal splenium and genu, respectively); whereas for the last (age and sex) matched group, G3 (N=8), the FOV was kept approximately parallel to such line ($\theta_{G3}=7\pm 8$ degrees). Note that θ_{G3} was statistically smaller (rank-sum tests, $P<1e-3$) than both θ_{G1} and θ_{G2} . Imaging equipment & protocol. All experiments were performed on a Siemens Verio 3T system with maximum gradient strength of 45 mT/m and a 32-channel head coil for reception. The DTI acquisition consisted of two averages of a twice-refocused, single-shot EPI² scan series with the following imaging parameters: TR/TE = [human: 12,700; phantom: 3,200]/81 ms; matrix, 128×128 [human: 72; phantom: 18] contiguous slices; voxel size: 2×2×2 mm³; EPI-echo spacing of 0.72 ms spacing; partial Fourier (phase) factor of 7/8; GRAPPA³ acceleration factor of 2 (38 reference lines), and receiver bandwidth set to [human: 1628/phantom: 1666 Hz/pixel]. The series was initiated with a T₂-weighted ($b=0$ s/mm² or $b0$) reference scan; followed by diffusion-weighted spin echo signals ($b\approx 1000$ s/mm²) sensitised along 30 non-collinear directions (Siemens default diffusion vectors with coordinates fixed to the xyz laboratory frame of reference); the total scan times were [human: 14'11"; phantom: 3'34"]. Data processing. FSL tools⁴ were used to correct for motion and eddy currents (first order only), fit the single tensor model and generate FA maps. (i) For the phantom experiment, a region of interest (ROI)—free of partial volume contamination (PVC)—was traced on a TA reference volume (see Fig. 1A). All remaining datasets were then rigidly aligned to the reference volume (using ANTs, <http://stnava.github.io/ANTs>) to infer DTI volume-specific ROI masks, from which mean FA values were extracted. Note that visual inspection ensured the transformed ROIs were all free of PVC. (ii) Mass-univariate TBSS⁵ with threshold free cluster enhancement⁶ (TFCE) was performed on whole-brain FA data to test the hypotheses that G3 differs from G1 and G2—over and above differences between G1 and G2. Statistical maps were thresholded at $P_{TFCE}<0.05$ controlling for the family-wise error (FWE) rate.

Results. Phantom experiment. An analysis of variance (ANOVA) for ROI FA distributions in N=14 TA measurements yielded no significant effect ($F=1.2$, $P>0.2$). A significant ANOVA group effect, however, was observed when comparing regional distributions across scan orientations ($F=30.7$, $P<1e-8$). Non-parametric post-hoc tests comparing mean regional FA values revealed statistically significant differences ($P<0.05$, Bonferroni corrected) between TA and TA-5 (see Fig. 1B). Human study. Fig. 1C shows TBSS results for the G1 vs. G3 contrast, which revealed strong, widespread differences (increased FA in G3) across the white matter skeleton. Highly concordant results were also obtained for the G2 vs. G3 contrast, whereas that for G1 vs. G2 returned no significant effects.

Discussion. It is presumed that DTI can probe tissue microstructure in a relatively rotationally invariant manner if the number of non-collinear diffusion encoding directions—assuming they are uniformly distributed—is at least 30^{7,8}. While this might be true in theory; in practice, many factors—including the complex interaction between imaging and diffusion gradients (which is FOV-positioning dependent), coregistration induced errors, and a large *et cetera*—may contribute to making DTI measurements rotationally variant. This hypothesis was tested with two experiments: first on a diffusion phantom, where the FOV was rotated 5 degrees away from the true axial orientation; and a human experiment, where two groups of subjects were scanned with slice alignments at steep angles (>15 degrees) from those in an otherwise matched group. **Conclusions:** Both experiments revealed significant differences in FA calculation across different orientations, which suggest that a standard DTI acquisition with standard processing steps is not a sufficiently robust recipe against systematic FOV and/or object/subject rotations. The human experiment, however, demonstrated that rotational dependencies can be suppressed if FOV/subject orientations are standardised at acquisition – as suggested by the negative G1 versus G2 contrast. It should be emphasised, as a corollary, that the present study does not invalid diffusion schemes with 30 uniformly-distributed directions. It argues, however, that the prescription of a large number of diffusion directions may not necessarily ensure unbiased results (with standard processing tools) if datasets are not acquired with certain consistency. More importantly, if FOV/subject orientation is not standardised, spurious results may often arise. This work warrants further investigation into the sources of the observed discrepancies and into possible solutions.

References: 1 Laun Proceedings ISMRM 2007. 2 Reese MRM 2003;49:177-182. 3 Griswold MRM 2002; 47:1202-1212 4 Smith et al, Neuroimage, 2004; 23 Suppl 1:S208-219. 5 Smith et al, Neuroimage, 2006; 31:1487-1505. 6 Smith et al, Neuroimage, 2009;44:83-98. 7 Batchelor MRM 2003; 49:1143-1151. 8 Jones MRM 2004; 51:807-815.

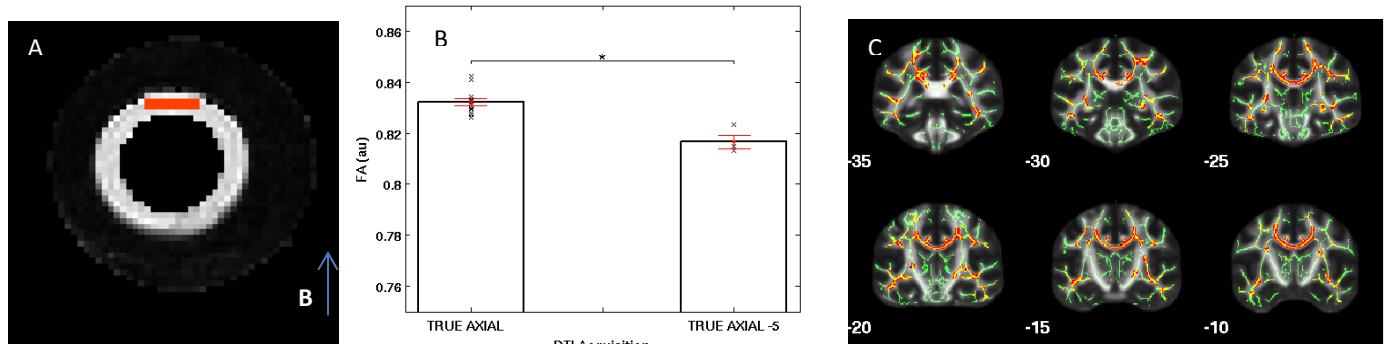


Figure 1. (A) Diffusion phantom's FA map - cross-sectional view (ROI in red). (B) Mean ROI FA values across FOV orientations. Bar plots and whiskers represent group means and standard errors, respectively. Statistically significant group difference ($P<0.05$) is denoted by (*). (C) TBSS group results for increased FA in G3 relative to G1 (FWE-corrected $P_{TFCE}<0.05$). Cluster-wise FA differences (red) are overlaid onto mean FA skeleton (green) and mean FA map in FMRIB58 space.